Chapter

# Dielectric Analysis Model for Measurement of Soil Moisture Water Content Using Electrical Capacitance Volume Tomography

*Mukhlisin Muhammad and Saputra Almushfi*

## Abstract

Electromagnetic methods have been widely used in the measurement of the water content of the soil. These methods utilize the permittivity as electrical properties of the soil, to determine the moisture content of the soil. Since the measurements are carried out indirectly, a calibration between permittivity and the water content of the soil is needed. Generally, the calibration method is generated by using an empirical and mixing model. This study presents a proposed model of calibration by using a normalization approach to calibrate the value of the permittivity of the water content of the soil. Then the model was applied using electrical capacitance volume tomography (ECVT) to image soil water content during infiltration of water in a soil column. Granular and silty sand were used as soil material in the experiments. The result showed that the model for measuring moisture water content can be seen in each layer during soil water infiltration in the soil column.

**Keywords:** dielectric analysis model, soil moisture water content, ECVT

## 1. Introduction

Measurement of soil moisture water content has become an important part of the analysis of various fields of study, especially those involving irrigation in agriculture, forestry, hydrology, and land activity. For example, in agriculture study, it is required to determine water source and ensure the quality of crop [1]. Moreover, soil moisture water content is useful to analyze soil water contamination by observing changes in water content during the addition of substance [2]. Soil water content also plays an important role in slope stability analysis [3–6].

Various techniques in the measurement of contamination and water content of soil have been discussed in literatures (e.g., [7–12]). Based on previous studies, soil water content measurement techniques are widely used as an electromagnetic method [13] such as time domain reflectometry [14], ground-penetrating radar (GPR) [8], and electrical capacitance [15]. These all methods measure the value of relative permittivity of soil to find soil moisture water content.

Tomography is a promising technique for measurement of water content in soil, especially for capacitance-based tomography. It is because this technique is not only capable of measuring water content in the soil but also is capable of imaging the

distribution of water in the soil. Tomography technique is also preferred because it is nondestructive and noninvasive. As a tomography technique, ECVT is a system used to view enclosed objects by measuring changes in capacitance and then compute relative permittivity distribution to create three-dimensional images in real time [16]. The shape of geometry sensor on ECVT is not confined to one form; it can be in the form of arbitrary shape of geometries [17]. This possibility gives an extra advantage of ECVT in measuring soil water content.

The previous study has successfully monitored the propagation of distribution of water in soil column [18]. In this study, the equation of normalized volumetric water content from ECVT method is proposed and compared with other equations. The proposed model is then used to analyze the volumetric water content during soil water infiltration in a vessel.

## 2. ECVT principle

The basic measurement of ECVT is derived from Poisson's equation:

$$\nabla \cdot (\varepsilon(x, y, z)\nabla\varphi(x, y, z) = -\rho(x, y, z)) \tag{1}$$

where $\varepsilon$ is relative permittivity distribution, $\phi$ is electric potential, and $\rho$ is charge distribution. From Eq. (1), capacitance value can be obtained by using the equation below:

$$C = \frac{1}{\Delta V}\oint_{\Gamma} \varepsilon(x, y, z)\nabla\varphi(x, y, z) \cdot \hat{n}\ \ dl \tag{2}$$

where $\Delta V$ is potential difference and $C$ is capacitance. By using matrix expression, Eq. (2) can be written like the following equation:

$$\mathbf{C} = \mathbf{S}\ \ \mathbf{G} \tag{3}$$

where **C** is capacitance matrix, **G** is distribution of relative permittivity matrix, and **S** is sensitivity matrix. The sensitivity matrix is generated from the sensor and geometry design and number of sensors. In matrix operation, the value of **G** can be obtained by inversing matrix **S** and multiplying it with matrix **C**. For non-square matrix, matrix inversion is very difficult to solve, so the approximation could be attempted by using transpose matrix. The equation to calculate matrix **G** becomes

$$\mathbf{G} = \mathbf{S}^{\mathbf{T}}\ \ \mathbf{C} \tag{4}$$

Equations (3) and (4) are known as the forward and inverse problem, respectively. Inverse problem is used to reconstruct the capacitance measurements to become relative permittivity distribution. The simple method for reconstruction is using linear back projection (LBP) [19].

## 3. Models of soil moisture water content and relative permittivity relationship

The relationship between relative permittivity and volumetric water content has been used by previous researchers to determine the volumetric water content. Many numbers of functions have been proposed to describe the ε-θ relationship

model across a range of soil water content. This model can be divided into two categories, which are model with one parameter and model with two or more parameters.

### 3.1 Model with one parameter

There are some models that proposed the ε-θ relationship. Topp et al. [20] introduced successfully the ε-θ relationship that is commonly used in geotechnical area. The relationship is as shown below:

$$\varepsilon = 3.03 + 9.3\theta + 146.0\theta^2 - 76.7\theta^3 \tag{5}$$

where $\varepsilon$ is the relative permittivity or dielectric constant and $\theta$ is the volumetric water content of soil.

Equation (1) is derived empirically through experiments of various of mineral soil using a time-domain reflectometer (TDR) at a frequency between 1 MHz and 1 GHz, with an estimated error value of 0.013 [20]. In another form, Topp's equation can also be written as follows:

$$\theta = -5.3 \times 10^{-2} + 2.92 \times 10^{-2}\varepsilon - 5.5 \times 10^{-4}\varepsilon^2 + 4.3 \times 10^{-6}\varepsilon^3 \tag{6}$$

In addition, Topp et al. [20] also proposed equations of ε-θ relationship for organic soil and 450 μm glass beads.

$$\varepsilon = 1.74 - 0.34\theta + 135\theta^2 - 55.3\theta^3 \quad \text{Organic soil} \tag{7}$$

$$\varepsilon = 3.57 + 31.7\theta + 114\theta^2 - 68.2\theta^3 \quad 450 - \mu\text{m glass beads} \tag{8}$$

Then Roth et al. [21] proposed another empirical equation by an experiment using miniprobe TDR which has been used previously by [22]. The ε-θ relationship for mineral soil proposed by [21] is

$$\theta = -0.0728 + 0.0448\varepsilon - 0.00195\,\varepsilon^2 + 0.000036\,1\varepsilon^3 \tag{9}$$

while the ε-θ relationship for organic soil and material is

$$\theta = \text{-}0.0233 + 0.0285\varepsilon - 0.000431\,\varepsilon^2 + 0.00000304\varepsilon^3 \tag{10}$$

Calibration of these equations has a volumetric water content error value of 0.015 $cm^3\ cm^{-3}$ for mineral soil and 0.035 $cm^3\ cm^{-3}$ for organic soil [22].

Simple equation of ε-θ relationship was proposed by [23]. This equation resulted from the principal of dielectric mixing models and analyzed the TDR without coatings that are considered potential sources of error in measurement:

$$\theta = 0.1181\sqrt{\varepsilon} - 0.1841 \tag{11}$$

Schaap et al. [24] also introduce a simple equation by performing experiments of 505 measurements of organic forest floor sample by using TDR where the ε-θ relationship is

$$\theta = 0.136\sqrt{\varepsilon} - 0.119 \tag{12}$$

The next equation comes from [25], which is using coaxial transmission system and using soil samples with wide range of soil textures:

$$\theta = -0.0286 + 0.02435\varepsilon - 0.0003421\varepsilon^2 + 0.00000237\varepsilon^3 \tag{13}$$

Equations (5)–(8) are used for measurement at a frequency of 100 MHz.

[13] proposed an empirical model where permittivity measurement was measured based on capacitance. This experiment used a type of quartz sand with a range of particle sizes between 0.15 and 0.9 mm:

$$\varepsilon = A\left(\frac{1}{1+(\alpha(1-\theta))^n}\right)^{1-\frac{1}{n}} + B \tag{14}$$

where A = 33, B = 2, α = 1.5, and n = 14.

### 3.2 Model with two or more parameters

Some relationship equations between permittivity and soil water content were also influenced by other parameters such as porosity and bulk density. By using the concept of mixing models and using data from others study [26–28], [29] proposed the following equations:

$$\varepsilon = \theta\left(\varepsilon_i + (\varepsilon_w - \varepsilon_i)\frac{\theta}{\theta_t}\gamma\right) + (\eta - \theta)\varepsilon_a + (1-\eta)\varepsilon_r \tag{15}$$

Equation (11) is used for $\theta \le \theta_t$, while $\theta > \theta_t$ used the following equation:

$$\varepsilon = \theta_t(\varepsilon_i + (\varepsilon_w - \varepsilon_i)\gamma) + (\theta - \theta_t)\varepsilon_w + (\eta - \theta)\varepsilon_a + (1-\eta)\varepsilon_r \tag{16}$$

where $\varepsilon_i$, $\varepsilon_w$, $\varepsilon_a$, and $\varepsilon_r$ are the permittivity of ice, water, air and rock, respectively (i.e., $\varepsilon_i$ = 3.2, $\varepsilon_w$ = 80, and $\varepsilon_a$ = 1), while $\theta_t$ is transition moisture (0.16–0.33), $\eta$ is the porosity of soil (0.5), and γ is the fitting parameter (0.3–0.5) [29].

In [30], the equation based on dielectric mixing model, which has been described by [31], is proposed. Experiments carried out by measuring a wide range of soil types using TDR with the error value of soil water content is not more than 0.013 $cm^3\ cm^{-3}$ [30], with forms of the equation below:

$$\theta = \frac{\varepsilon^\gamma - (1-\eta)\varepsilon_s^\gamma - \eta\varepsilon_a^\gamma}{\varepsilon_w^\gamma - \varepsilon_a^\gamma} \quad ; \gamma = -1 \tag{17}$$

$$\theta = \frac{\varepsilon^\gamma - (1-\eta)\varepsilon_s^\gamma - \eta\varepsilon_a^\gamma}{\varepsilon_w^\gamma - \varepsilon_a^\gamma} \quad ; \gamma = 1 \tag{18}$$

where γ = −1 for three phases in series and γ = 1 for three phases in parallel.

Another model is proposed by [32]. They conducted the experiments by using TDR and 62 kinds of soil sample that consist of mineral soils, organic soil, standard pot soils, artificial peat loess and peat sand, sea and river sand, forest litter, etc. which differ in terms of texture and bulk density [32].

$$\theta = \frac{\sqrt{\varepsilon} - 3.47 + 6.22\eta - 3.82\eta^2}{7.01 + 6.89\eta - 7.83\eta^2} \tag{19}$$

Equation (13) gives the uncertainty of soil water content value of 0.03.

Gardner et al. [15] used capacitance measurement methods to obtain soil water content with the soil dry bulk density values ranging between 1.08 and 1.49, then

using multiple linear regression analysis to best fit the measurement data, resulting in the following equation:

$$\theta = \frac{\sqrt{\varepsilon} + 1.208 - 2.454\rho}{9.93} \tag{20}$$

where $\rho$ is dry bulk density.

Robinson et al. [14] give the equation used for coarse-textured, layered soils by using TDR and coarse-grained, glass bead, and quartz grains:

$$\theta = \eta\left(\frac{\sqrt{\varepsilon} - \sqrt{\varepsilon_{dry}}}{\sqrt{\varepsilon_{sat}} - \sqrt{\varepsilon_{dry}}}\right) \tag{21}$$

where $\varepsilon_{dry}$ and $\varepsilon_{sat}$ are the permittivity measured at oven dry soil and saturation soil (**Table 1**).

### 3.3 Comparison using existing data

Data from previous research (e.g., [20, 21, 25–27, 29, 31–35]) are used to compare the patterns of the equations which are discussed in this study. This data consists of various soil types with different properties.

**Figure 1** shows several curves representing Eqs. (5)–(14). All equations look occupied by all the available data. However, each equation appears to have certain characteristics to the data. Eqs. (8) and (12) only cover the boundary area of the data, while the other equations lie mostly in the central part of the data. These would seem to depend on the properties of the soil types used. One of the characteristics analyzed in this study is the porosity of the soil.

**Figure 2** shows the influence of porosity ($\eta$ = 0.3 to $\eta$ = 0.7), on the suitability of the equations (Eqs. (15), (16), (18) and (19)–(21)) with data, and also displayed some of the data with a value of porosity (0.33, 0.44, and 0.62) in order to see the effect of porosity on predictions of water content of the equation. From the image it can be seen that the different porosity values of the data will result in different patterns.

In **Figure 2a**, the equations already have the same pattern with the data, but a change of porosity in the equation does not give a significant effect on the pattern of the line, so it is only fit in certain small area of data though with different porosity.

**Figure 2b** shows that the equation is such as the linear equation that has not affected on the changes in porosity. These equations also appear not to follow the pattern of distribution of data. The same thing happened in **Figure 2c** with a shift in values on the x-axis which is more to the left.

An overestimated result is produced in **Figure 2e**, where the equation is not able to cover all areas of data; whereas in **Figure 2f**, it has been seen covering almost all areas except the data on water content values smaller than 0.2, but this equation has not been able to adjust to the data that have a value of porosity. The only equation that gives the better approach is **Figure 2d**. This equation produces a pattern in accordance with the existing data. The equation is also seen fit to data that has a value of porosity.

In this study the relative permittivity was analyzed by the ECVT system generated in the form of normalization. Normalized volumetric water content can be defined as

$$\Theta = \frac{\theta - \theta_r}{\theta_s - \theta_r} \tag{22}$$

| Eq. | Source | Experimental method | Soil type | Properties of soil | | |
|---|---|---|---|---|---|---|
| | | | | Porosity ($cm^3\ cm^{-3}$) | Bulk density ($g\ cm^{-3}$) | Particle density ($g\ cm^{-3}$) |
| Model with one parameter | | | | | | |
| (5) | [20] | ε: using TDR Tektronix 7S12 model to perform 18 experiments with different treatments<br>θ: using gravimetric technique | • Mineral soil<br>• Organic soil<br>• Vermiculite<br>• Glass beads | — | • 1.04–1.44<br>• 0.422<br>• 1.08<br>• 1.49–1.61 | — |
| (6) | | | | | | |
| (7) | | | Organic soil | — | 0.422 | — |
| (8) | | | 450 μm glass beads | — | 1.60–1.61 | — |
| (9) | [21] | ε: TDR miniprobe 250 ps rise-time needle pulse<br>θ: gravimetric technique | 9 mineral soils | 0.418–0.482 | 1.26–1.55 | 2.28–2.67 |
| (10) | | | 7 organic soils | 0.527–0.785 | 0.2–0.77 | 0.70–1.63 |
| (11) | [23] | Using model of inverse averaging for TDR method by analyzing the mixing model | — | — | — | — |
| (12) | [24] | ε: TDR Tektronix 1502B<br>θ: gravimetric technique | 25 samples of forest floors | — | 0.086–0.263 | 1.3 |
| (13) | [25] | Coaxial transmission/reflection apparatus controlled by a Hewlett-Packard 8510C Vector Network Analyzer system 45 MHz to 26.5 GHz | — | — | — | — |
| (14) | [13] | ε: based on capacitance measurement<br>θ: gravimetric technique | Quartz sand | — | — | — |
| Model with two or more parameters | | | | | | |
| (15) | [29] | Modeling by using data from other studies [26–28] | 22 different samples | 0.4–0.6 | 1.1–1.7 | 2.6–2.75 |
| (16) | | | | | | |
| (17) | [30] | TDR | From 11 different field sites | | | |
| (18) | | | | | | |
| (19) | [32] | TDR CAMI | 62 kinds of soil samples | 0.33–0.95 | 0.13–1.66 | 1.06–2.7 |
| (20) | [15] | Capacitance probe 80–150 MHz | • Brown earths<br>• Silica materials | — | • 1.08–1.49<br>• 1.24–1.63 | — |
| (21) | [14] | TDR Tektronix 1502B | Coarse-grained, quartz grain, sandy soil | — | — | — |

**Table 1.**
*Summary of all equations of ε-θ relationship.*

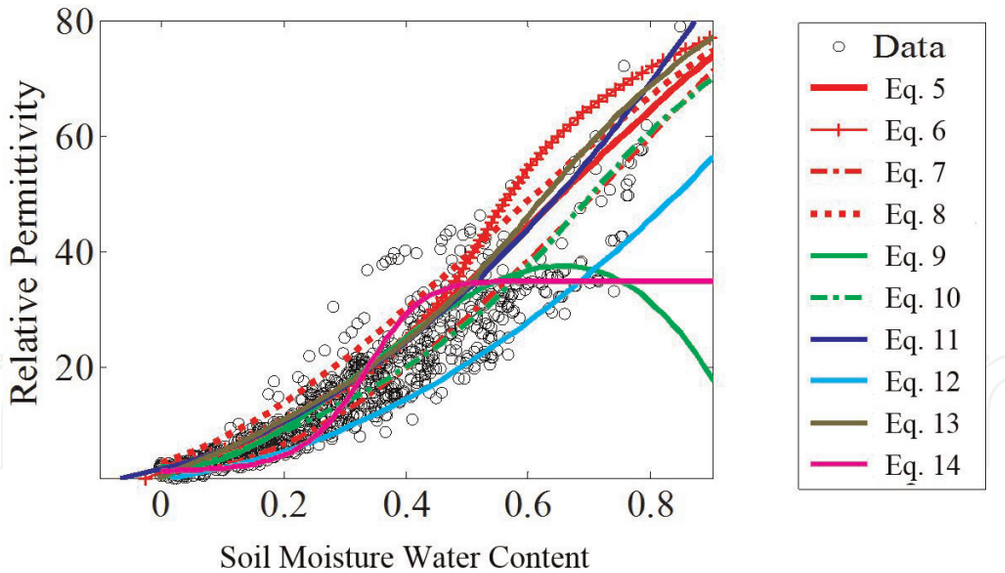


**Figure 1.**
*Comparisons using all data for Eqs. (5)–(14).*

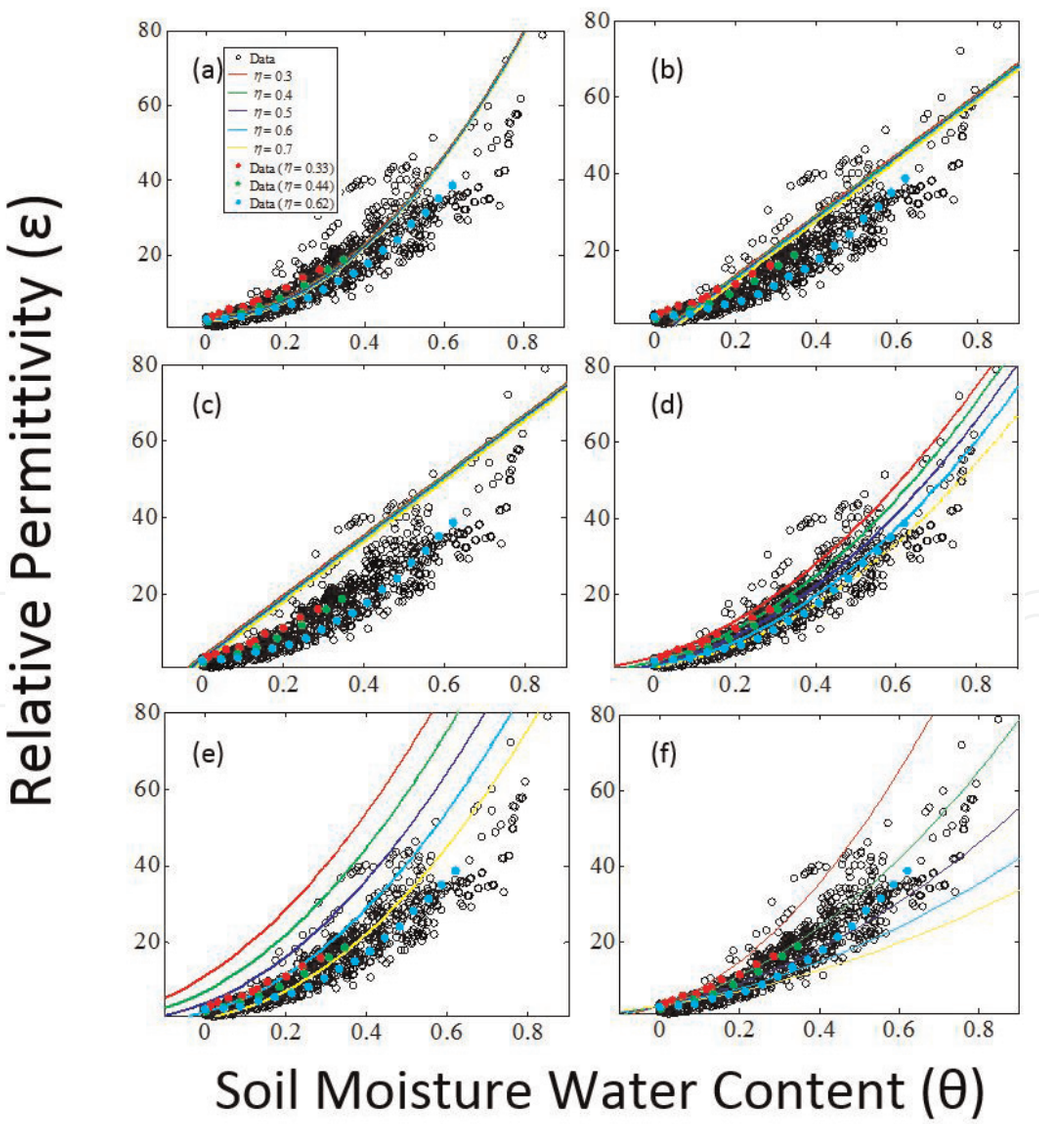


**Figure 2.**
*Comparison all equations with different porosity, by using: a) Eq. 15; b) Eq. 16; c) Eq. 18; d) Eq. 19; e) Eq. 20; f) Eq. 21.*

| Material | Relative permittivity | Elements |
|---|---|---|
| Air | 1 | $N_2$, $O_2$ |
| Water | 80 | $H_2O$ |
| Dry soil | 3–10 | N, P, K, Ca, Mg, S, Cu, Zn, Fe, Mn, B, Cl, Na, H |

**Table 2.**
*Material properties.*

where $\theta$ is the volumetric water content, $\theta_r$ is the residual volumetric water content, and $\theta_s$ is the saturated volumetric water content.

The normalization of relative permittivity gives privilege to define normalized volumetric water content, in this study it is assumed in three models:

$$\begin{aligned} \Theta &= \varepsilon_N{}^{0.5} && \text{(a)} \\ \Theta &= \varepsilon_N && \text{(b)} \\ \Theta &= \varepsilon_N{}^{2} && \text{(c)} \end{aligned} \tag{23}$$

where $\varepsilon_N$ is normalized permittivity which can be calculated as

$$\varepsilon_N = \frac{\varepsilon - \varepsilon_{air}}{\varepsilon_{water} - \varepsilon_{air}} \tag{24}$$

where $\varepsilon$, $\varepsilon_{air}$, and $\varepsilon_{water}$ are actual relative permittivity measurement, relative permittivity of air, and relative permittivity of water, respectively (**Table 2**).

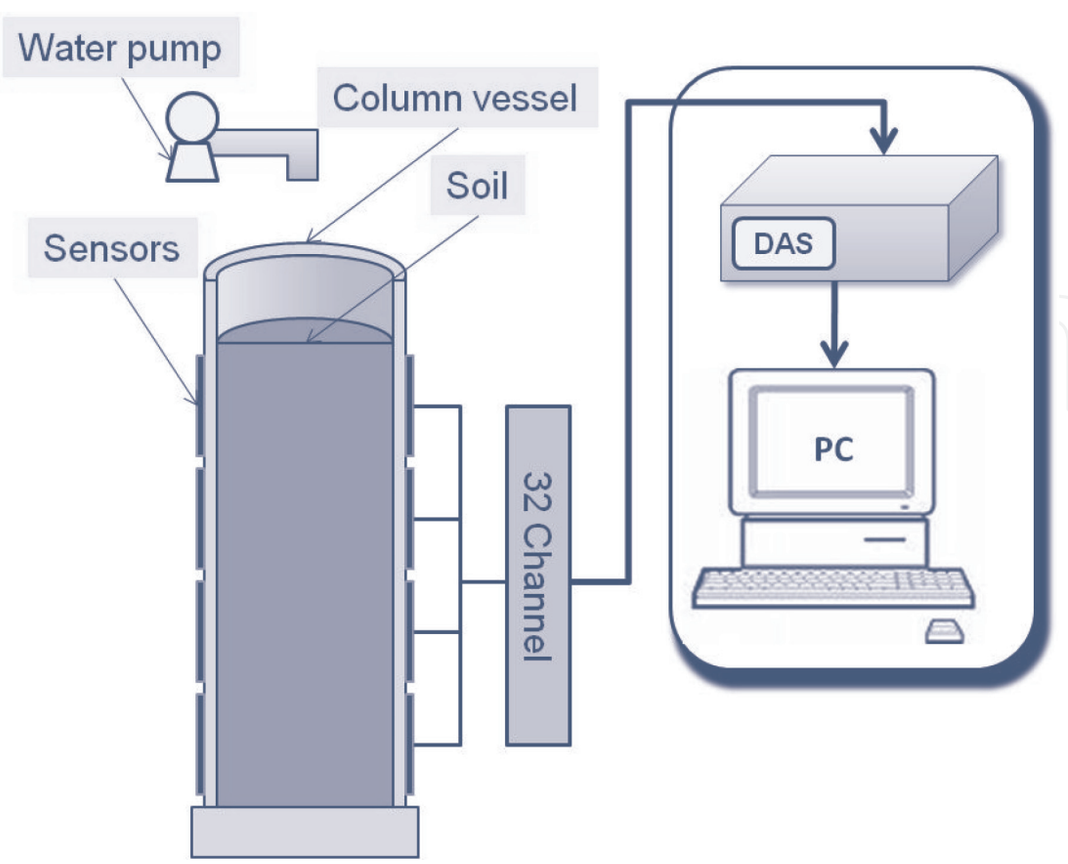


**Figure 3.**
*Experimental setup [15].*

## 4. Experimental setup

ECVT system consists of three parts: (i) sensors, (ii) data acquisition, and (iii) system reconstruction and visualization as shown in **Figure 3**. In this experiment we used 32 channel hexagonal sensors for the first experiment and 24 channel hexagonal sensors for the second experiment, as a soil column with diameter and height 11.5 and 27 cm, respectively. This column is divided into 32 layers with the 1st layer as the top layer and 32nd layer as the bottom layer.

In the first experiment, 3 l by volume of soil in the column was supplied. The soil material that was used in this study was sand collected from the Cisadane River in Tangerang, Indonesia. The soil contained 17% fine sand and 83% medium sand with porosity of soil 41.79%. The specific gravity and soil density were 2.663 and 1.55 g $cm^{-3}$, respectively. In this experiment, the soil in the vessel was supplied with water flow with a discharge of 7.2 ml/s until ponded condition, and the discharge was stopped when the pond of water level was at 2 cm above the surface soil. During ponded condition, the data capacitances were measured iteratively and sent to the computer. The data acquisition frequency was set to one frame per second.

In the second experiment, 3 kg of silty sand was supplied into the column. After that, 1.4 liter of water was filled into the soil column using constant head method, in which height of the water is maintained constant by a distance of 4 cm from the surface of soil.

## 5. Result and discussion

Normalized volumetric water content and relative permittivity relationship of several equations is shown in **Figure 4**. The first model of the proposed model seems to have a similar pattern with Topp et al. [20] and Malicki et al. [32] models. By adding some constants value to the first model, this model will be quite fit with

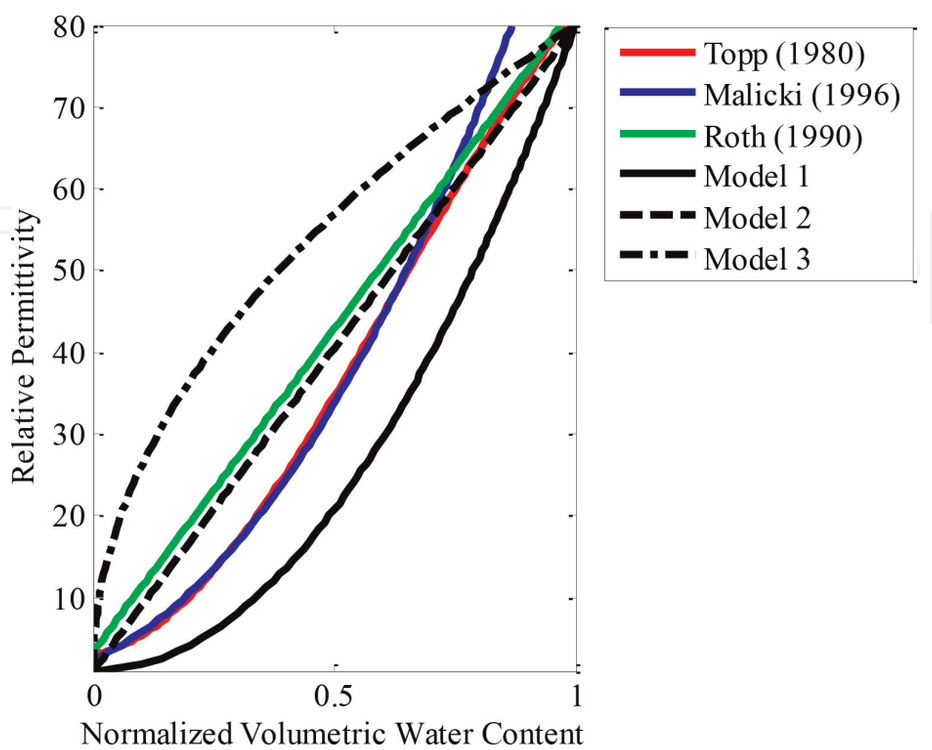


**Figure 4.**
*Normalized volumetric water content and relative permittivity relationship of the three proposed models compared with established models.*

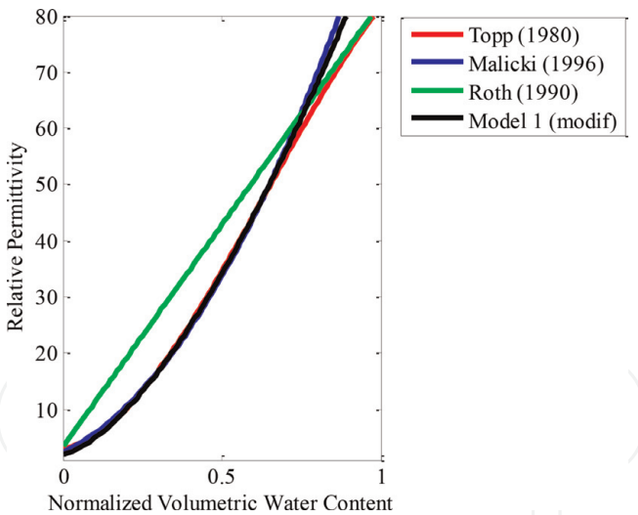


**Figure 5.**
*Normalized volumetric water content and relative permittivity relationship of the first model modification compared with established models.*

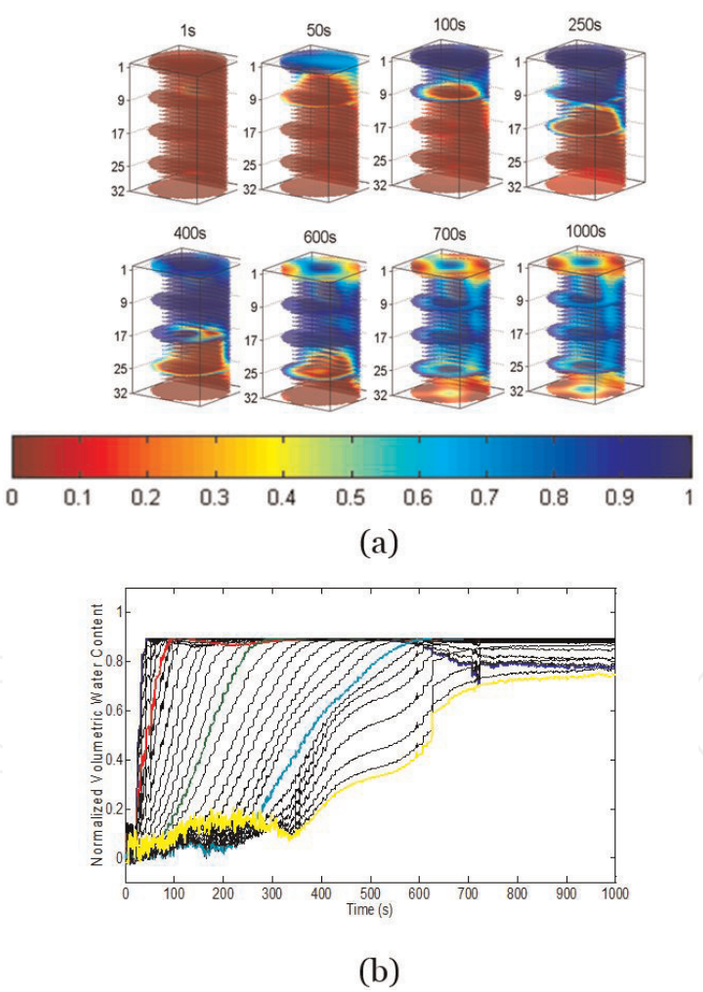


**Figure 6.**
*Result from experiment 1, soil water infiltration (a) and normalized volumetric water content of soil (blue line, 1st layer; red line, 9th layer; green line, 17th layer; cyan line, 25th layer; and yellow line, 32nd layer) (b).*

Topp and Malicki models. However, the second model looks similar to Roth et al. [21] model, which gives a linear relationship between normalized volumetric water content and relative permittivity. In contrast, the third model is out of fit with other models.

Modification to the first model (Eq. (23a)) to fit with previous models can be done by adding the constants by trial and error. The modification is shown below:

$$\Theta = 0.9 \times (\varepsilon_N\text{-}0.015)^{0.65} \tag{25}$$

**Figure 5** shows the first model with modification (Eq. (25)) quite fit with the Topp and Malicki models.

Based on this result, Eq. (25) was used to analyze the normalized volumetric water content during water infiltration in soil. The results of water infiltration in soil can be seen in **Figure 6**. **Figure 6a** shows the images of normalized volumetric water content from red (i.e., dry condition, $\varepsilon_N$ = 0) to blue (i.e., saturated condition, $\varepsilon_N$ = 1) colors. The scale of the color means normalization value of relative permittivity distribution in image.

**Figure 6a** shows the image sequencing of water infiltration methods from 1, 50, 100, 250, 400, 600, 700, and 1000 s, respectively. In this figure, the position and movement of water per second can be seen clearly. **Figure 6b** shows normalized

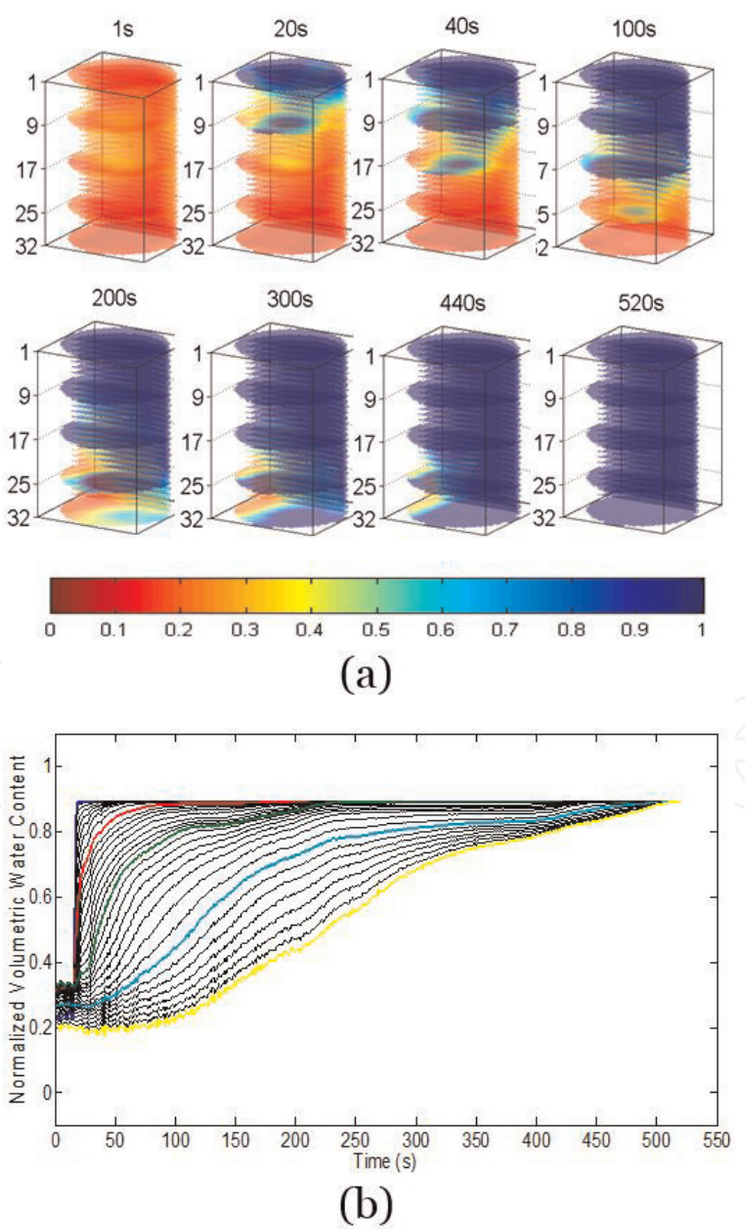


**Figure 7.**
*Result from experiment 2, soil water infiltration (a) and normalized volumetric water content of soil (blue line, 1st layer; red line, 9th layer; green line, 17th layer; cyan line, 25th layer; and yellow line, 32nd layer) (b).*

volumetric water content of soil for 32 layers during water infiltration in the soil. Blue, green, red, cyan, and yellow lines indicated 1, 9, 17, 25, and 32 soil layers, respectively. In the first layer, the normalized volumetric water content increases very fast and reaches a saturated condition at around 100–300 s. The degree of saturation for 1st layer starts to decrease after supplying of water was stopped at 300 s and relative constant was at around 0.3 from 700 to 1000 s. For 9th and 17th layers, the degree of saturation increases sequencing and reaches a saturated condition at a similar time (i.e., at around 450 s) and starts to decrease at 500 s, while for the 25th layer, the degree of saturation increases at around 300 s and reaches a stable condition at 700 s with a degree of saturation at around 0.85. Moreover at the 32nd layer, the degree of saturation increases at 630 s, and the degree of saturation reaches 0.2 at the end of the experiment (i.e., 1000 s). This experiment showed clearly the availability of air trapped at the bottom of soil in the vessel (see **Figure 6a**).

**Figure 7** also shows the image sequencing of water infiltration (**Figure 7a**) and normalized volumetric water content of each layer of the soil column (**Figure 7b**). In **Figure 7a**, it can be seen that the silty sand has a normalized relative permittivity value around 0.3 before water infiltrate to the soil column. It can be caused by two possibilities, (i) because of the moisture content stored in the soil and (ii) because the soil particles are very small and compact, so the porosity of soil is also small which causes no air cavity in the soil. From **Figure 7b** we can see how the water infiltrates into the each layer clearly. The first layer has increased drastically around the first 30 s. It is easily understood that the top layers will reach the maximum value of normalized volumetric water content first, because these layers get the first supply of water.

## 6. Conclusion

Some equations between the relative permittivity and volumetric water content have been described in this study. From this study, there is an equation that has demonstrated efficacy in conformity with the data of experimental results, that is, equation proposed by [32]. This equation uses the porosity factor as a parameter in the relationship between volumetric water content and relative permittivity.

Normalized volumetric water content of soil has been analyzed in this study using ECVT system. Normalized volumetric water content can be shown and analyzed layer per layer of soil column for every second. We found that the ECVT system has advantages in measuring soil water content which are nondestructive and noninvasive to the sample object, 3D image, and real-time monitoring for water infiltration.

## Acknowledgements

The authors wish to thank the Ministry of Research, Technology and Higher Education of Republic of Indonesia, for providing the research grand.

## Conflict of interest

The authors declare that there is no conflict of interest.

## Author details

Mukhlisin Muhammad[1*] and Saputra Almushfi[2]

1 Politeknik Negeri Semarang, Semarang, Indonesia

2 CTECH Labs Edwar Technology, Tangerang, Indonesia

*Address all correspondence to: mmukhlis2@gmail.com

## References

[1] Moroizumi T, Hamada H, Sukchan S, Ikemoto M. Soil water content and water balance in rainfed fields in Northeast Thailand. Agricultural Water Management. 2009;**96**(1):160-166

[2] Kottler BD, White JC, Kelsey JW. Influence of soil moisture on the sequestration of organic compounds in soil. Chemosphere. 2001;**42**(8):893-898

[3] Osman N, Barakbah SS. Parameters to predict slope stability—Soil water and root profiles. Ecological Engineering. 2006;**28**(1):90-95

[4] Mukhlisin M, Taha MR, Kosugi K. Numerical analysis of effective soil porosity and soil thickness effects on slope stability at a hillslope of weathered granitic soil formation. Geosciences Journal. 2008;**12**(4):401-410

[5] Mukhlisin M, Taha MR. Slope stability analysis of a weathered granitic hillslope as effects of soil thickness. European Journal of Scientific Research. 2009;**30**(1):36-44

[6] Mukhlisin M, Baidillah MR, Taha MR, El-Shafie A. Effect of soil water retention model on slope stability analysis. International Journal of Physical Sciences. 2011;**6**(19):4629-4635

[7] Topp GC. State of the art of measuring soil water content. Hydrological Processes. 2003;**17**(14): 2993-2996

[8] Huisman JA, Hubbard SS, Redman JD, Annan AP. Measuring soil water content with ground penetrating radar: A review. Vadose Zone Journal. 2003; **2**(4):476-491

[9] Basinger JM, Kluitenberg GJ, Ham JM, Frank JM, Barnes PL, Kirkham MB. Laboratory evaluation of the dual-probe heat-pulse method for measuring soil water content. Vadose Zone Journal. 2003;**2**(3):389

[10] Gaskin GJ, Miller JD. Measurement of soil water content using a simplified impedance measuring technique. Journal of Agricultural Engineering Research. 1996;**63**(2):153-159

[11] Ramírez V, Sánchez JA, Hernández G, Solís S, Torres J, Antaño R, et al. A promising electrochemical test for evaluating the hydrocarbon-type pollutants contained in industrial waste soils. International Journal of Electrochemical Science. 2011;**6**(5): 1415-1437

[12] Ruíz C, Anaya J, Ramírez V, Alba GI, García MG, Carrillo-Chávez A, et al. Soil Arsenic Removal by a Permeable Reactive Barrier of Iron Coupled to an Electrochemical Process. 2011

[13] Wu SY, Zhou QY, Wang G, Yang L, Ling CP. The relationship between electrical capacitance-based dielectric constant and soil water content. Environment and Earth Science. 2011; **62**(5):999-1011

[14] Robinson DA, Jones SB, Wraith JM, Or D, Friedman SP. A review of advances in dielectric and electrical conductivity measurement in soils using time domain reflectometry. Vadose Zone Journal. 2003;**2**(4):444-475

[15] Gardner CMK, Dean TJ, Cooper JD. Soil water content measurement with a high-frequency capacitance sensor. Journal of Agricultural Engineering Research. 1998;**71**(4):395-403

[16] Warsito W, Marashdeh Q, Fan L-S. Electrical capacitance volume tomography. IEEE Sensors Journal. 2007;**7**(4):525-535

[17] Warsito W, Marashdeh Q, Fan LS. Real time volumetric imaging of multiphase flows using electrical capacitance volume-tomography

(ECVT). In: 5th World Congress in Industrial Process Tomography; 2007. pp. 755-760

[18] Mukhlisin M, Baidillah MR, El-Shafie A, Taha MR. Real time monitoring of soil water infiltration using electrical capacitance volume-tomography (ECVT). In: 4th International Conference on Water Resources and Arid Environments (ICWRAE 4); 2010. pp. 749-756

[19] Yang WQ, Spink DM, York TA, McCann H. An image-reconstruction algorithm based on Landweber's iteration method for electrical-capacitance tomography. Measurement Science and Technology. 1999;**10**(11): 1065-1069

[20] Topp GC, Davis JL, Annan AP. Electromagnetic determination of soil water content: Measurements in coaxial transmission lines. Water Resources Research. 1980;**16**(3):574-582

[21] Roth CH, Malicki MA, Plagge R. Empirical evaluation of the relationship between soil dielectric constant and volumetric water content as the basis for calibrating soil moisture measurements by TDR. Journal of Soil Science. 1992; **43**(1):1-13

[22] Malicki MA, Plagge R, Renger M, Walczak RT. Application of time-domain reflectometry (TDR) soil moisture miniprobe for the determination of unsaturated soil water characteristics from undisturbed soil cores. Irrigation Science. 1992;**13**(2): 65-72

[23] Ferré PA, Rudolph DL, Kachanoski RG. Spatial averaging of water content by time domain reflectometry: Implications for twin rod probes with and without dielectric coatings. Water Resources Research. 1996;**32**(2):271-279

[24] Schaap MG, de Lange L, Heimovaara TJ. TDR calibration of organic forest floor media. Soil Technology. 1997;**11**(2):205-217

[25] Curtis JO. Moisture effects on the dielectric properties of soils. IEEE Transactions on Geoscience and Remote Sensing. 2001;**39**(1):125-128

[26] Lundien JR. Terrain Analysis by Electromagnetic Means. Vicksburg, MS: U.S. Army Engineer Waterways Experiment Station; 1971

[27] Newton RW. Microwave Remote Sensing and its Application to Soil Moisture Detection. College Station, TX: Texas A&M University, College Station; 1977

[28] Wang J, Schmugge T, Williams D. Dielectric constants of soils at microwave frequencies—II. National Aeronautics and Space Administration Technical Paper. 1978

[29] Wang JR, Schmugge TJ. An empirical model for the complex dielectric permittivity of soils as a function of water content. IEEE Transactions on Geoscience and Remote Sensing. 1980;**GE-18**(4):288-295

[30] Roth K, Schulin R, Fluhler H, Attinger W. Calibration of time domain reflectometry for water content measurement using a composite dielectric approach. Water Resources Research. 1990;**26**:2267-2273

[31] Dobson MC, Ulaby FT, Hallikainen MT, El-Rayes MA. Microwave dielectric behavior of wet soil—Part II: Dielectric mixing models. IEEE Transactions on Geoscience and Remote Sensing. 1985; **GE-23**:35-45

[32] Malicki MA, Plagge R, Roth CH. Improving the calibration of dielectric TDR soil moisture determination taking into account the solid soil. European Journal of Soil Science. 1996;**47**:357-366

[33] Friedman SP. A saturation degree-dependent composite spheres model for

describing the effective dielectric constant of unsaturated porous media. Water Resources Research. 1998;**34**: 2949-2961

[34] Hilhorst MA, Dirksen C, Kampers FWH, Feddes RA. New dielectric mixture equation for porous materials based on depolarization factors. Soil Science Society of America Journal. 2000;**64**:1581-1587

[35] Robinson DA, Jones SB, Blonquist JM, Friedman SP. A physically derived water content/permittivity calibration model for coarse-textured, layered soils. Soil Science Society of America Journal. 2005;**69**:1372-1378